Laboratory investigation of hygrothermal monitoring of hempconcrete walls

Soudani, L, Fabbri, A, McGregor, F & Morel, J-C

Original citation:
Soudani, L, Fabbri, A, McGregor, F & Morel, J-C 2017, 'Laboratory investigation of hygrothermal monitoring of hempconcrete walls' *Rilem Technical Letters*, vol 2, pp. 20-26
https://dx.doi.org/10.21809/rilemtechlett.2017.36

DOI 10.21809/rilemtechlett.2017.36
ISSN 2518-0231

Publisher: Rilem

RILEM Technical Letters (2017) 2: 20-26
DOI: http://dx.doi.org/10.21809/rilemtechlett.2017.36

Laboratory investigation of hygrothermal monitoring of hemp-concrete walls

Lucile Soudani [a], Antonin Fabbri [a*], Fionn McGregor [a], Jean-Claude Morel [b]

[a] LGCB-LTDS, UMR 5513 CNRS, ENTPE, Université de Lyon, 69100 Vaulx-en-Velin, France
[b] Research Centre in Low Impact Buildings, Faculty of Engineering, Environment & Computing, Coventry University, West Midlands, UK

Received: 04 July 2017 / Accepted: 23 October 2017 / Published online: 19 November 2017

Abstract

In the global will of reducing fossil energy consumption and greenhouse gas emission in the building sector, the use of bio-based insulating materials is gaining interest thanks to their profitable properties and their suitability for the renovation of ancient buildings made out of unconventional materials. However, such materials are still lacking of characterization, and more precisely of on-site evaluation, as no complete measurement protocol is available. The starting point to fill this gap would be to set-up a protocol for whole building instrumentation, and this paper is investigating questions arisen in that goal, and more precisely regarding the impact of sensor locations on the assessment of key parameters. For that purpose, instrumented polystyrene and hemp concrete wallets of dimensions $0.9 \times 0.9 \times 0.1$ m^3 with well-known thermal and hydric characteristics are tested within a double climatic chamber. The impact of temperature sensor locations and implementations are tested through indirect estimation of the thermal conductivities of the materials composing the wallets. The effect of the hygrothermal processes on the measurement of thermal performance is also investigated through the analysis of the wall global transmittance. These results finally allow to provide some recommendations concerning the on-site instrumentation of hemp concrete walls.

Keywords: Hemp concrete; Instrumentation; Thermal transmittance

1 Introduction

The energy cost of buildings is due to their consumptions (heat, ventilation…), but also to the embodied energy required for their construction, their rehabilitation as well as their dismantling. In this context, the use of bio-based insulating materials like hemp concrete is gaining interest. Indeed, they allow to drastically reduce fossil energy consumption and greenhouse gas emissions associated with the manufacture compared to conventionally used materials for building insulation such as rock wool or fiberglass [1].

They are renewable, extracted from biomass and have promising thermal and acoustical characteristics [2–5]. In addition, thanks to their ability to allow diffusion of water vapor within their porous network [6], these materials present an alternative option to isolate and rehabilitate buildings made with non-industrial materials (rammed earth, cob, adobe,…) and whose stability requires to maintain a water exchange with the outside [7–10].

Their permeability to vapor, when combined with their strong affinity with water molecules, make them hygroscopic materials [11]. In other terms, they may be used as passive regulation systems of indoor air relative humidity, which is very important for building occupants as it can significantly influence their comfort, health, and productivity. Indeed, extremely low levels of relative humidity (below 20%) may cause eye or skin irritations and dry the nasal mucous membranes, resulting in a higher risk of respiratory infections. On the other hand, high levels of relative humidity may lead to the development of fungi, which can cause allergies as manifested by asthma and rhinitis [12,13], and the emission of volatile organic compounds is favored [14]. Nowadays, there is consensus that indoor relative humidity should remain between 40% and 60%. At building scale, it was shown that the use of hygroscopic materials leads to a significant reduction of moisture variation amplitudes, which thus induces energy savings on ventilation [15].

The thermal conductivity of hemp concrete depends on its formulation, its implementation and its water content. When it is measured in laboratory, it commonly ranges from 70 mW·m^{-1}·K^{-1} to 300 mW·m^{-1}·K^{-1} [16], which is quite high for an insulating material. In comparison, the thermal conductivities of expended polystyrene and glass wool are

*Corresponding author: Antonin Fabbri, E-mail: antonin.fabbri@entpe.fr

about 40 mW·m^{-1}·K^{-1}. However, the thermal performance of hygroscopic insulating systems such as hemp concrete is commonly above what can be expected when only their thermal conductance and thickness are considered. These higher performances can be attributed to the latent heat associated with the liquid-to-vapor phase change of the water located in the porous network of the material. An increasing number of research publications focuses on assessing these phenomena within hygroscopic walls and modeling them [17,18]. It leads to the development by the scientific community of a fairly high number of codes and procedures. One of the more visible studies in this field was conducted within the HAMSTAD project (cf. the series of publication in *Journal of Thermal environment* and *Building Science* n° 27 in 2004, and in particular [19]). But, most of the studies remains either theoretical and/or at the laboratory scale, while on-site analysis at the building scale would be necessary to clearly assess the real impact of hygroscopic materials on the building performance. The first reason can be the in-situ material properties, as well as the testing conditions, which are potentially very different from those estimated in the laboratory, in particular since the inhabitants' behavior is difficult to predict and/or record. Secondly, the interactions and couplings between the several elements composing the building are still not totally understood.

In order to fill this gap, the starting point would be to set up a proper instrumentation protocol for buildings with hygroscopic materials. Indeed, even if few studies expose some feedback on ambiances and walls instrumentations [20–23], no clear assessment is made on the influence of sensor types and/or positions.

In this context, this paper aims at clarifying some experimental methodology and precautions to consider for the instrumentation of hygroscopic walls. For that purpose, instrumented polystyrene and hemp concrete wallets of dimensions 0.9 × 0.9 × 0.1 m^3 with well-known thermal and hydric characteristics are tested within a double climatic chamber. The impact of temperature sensor locations and implementations are tested through indirect estimation of the thermal conductivities of the materials composing the wallets. The effect of the hygrothermal processes on the measurement of thermal performance is also investigated through the analysis of the wall global transmittance. These results finally allow to provide some recommendations concerning the on-site instrumentation of hemp concrete walls.

2 Materials and methods

2.1 Studied materials

The binder used in this study is the CalcoBlanc from ParexLanko. It is mixed with water and hemp with a hemp to binder mass ratio of 0.33 and a water to binder mass ratio of 0.88. The mixture is then compacted in 8 successive layers within a framework whose internal dimensions are 0.9 × 0.9 × 0.10 m^3. The average wet density after manufacture was 700 kg·m^{-3}. One of the wall surfaces is coated with a 2 cm thick lime-sand plaster.

In addition to the wall, the same batch was used to realize cylindrical samples (diameter of 16cm and length of 32 cm) and plates (0.3 × 0.3 × 0.06 m^3). These samples were used for porous, hydric and thermal laboratory characterizations. The wet density of these samples just after fabrication was the same as the wall's one. The apparent dry density of the hemp concrete, ρ_d, is measured from the weighting of the cylinders dried at 60°C, and the porosity, ϕ is estimated with a nitrogen pycnometer (Ultrapyc 1200e), through the relation : $\phi = (\rho_s - \rho_d)/\rho_s$, where ρ_s is the density of the skeleton estimated with the pycnometer. It leads to ρ_d =440 kg·m^{-3}, ρ_s =2095 kg·m^{-3} and ϕ =79%. The hydric characterization consists in an isothermal sorption isotherm following the NF EN ISO 12571 standard at 20°C. It leads to a linearized moisture capacity of 15.8 kg/m^3 when the relative humidity is between 30% and 80%. The water vapor resistance (μ) was estimated with the wet and dry cup methods. The wet cup method consisted in placing the sample on top of a box containing a salt solution of Potassium Chloride to maintain a RH level of 85%. Silica gel was used for the dry cup method to maintain a RH level of 5%. The samples with its box were then stored in a climatic chamber maintained at a RH level of 50% and a temperature of 23°C. The data analysis was made following the methodology presented in [24]. It consists in taking into account a correction due to the skin effect of the tested material, which is quantified from the diffusion tests on samples of at least three different thicknesses. At the end, the value of the water vapor resistance factor was found to be same and equal to 3.4 for these three conditions. It follows that the coefficient of permeability of liquid water in this range of relative humidity can be assumed to be null [25]. Finally, the thermal conductivity, λ, is measured with a hot wire apparatus (Neotim - FP2C) which was found to give similar results than a hot plate apparatus (HFM - Netsch) on a similar hemp concrete material [26]. It leads to a dry thermal conductivity of 135 mW·m^{-1}·K^{-1}.

In addition to the hemp concrete wall, calibration tests were made on an expanded polystyrene wall whose thermal properties are known to be equal to λ = 40 mW·m^{-1}·K^{-1} and ρC = 24 kJ·m^{-3}·K^{-1}.

2.2 Test conditions and instrumentation scheme

The walls were tested in a double climatic chamber that allows the regulation of temperature and relative humidity on each side of the wall, independently to each other. Their instrumentations are illustrated in Figure 1.

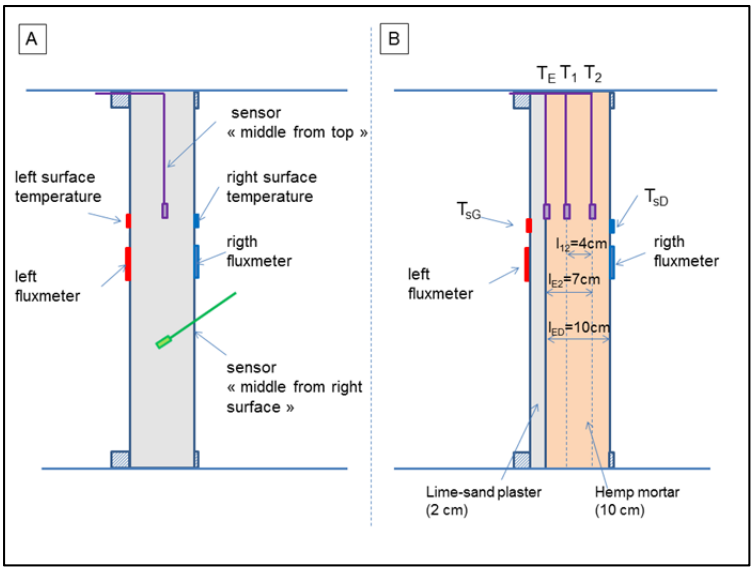

Figure 1. Schematic representation of the sensors set up in tested wallets: (A) polystyrene wallet; (B) hemp concrete wallet + lime-sand plaster

Two temperature sensors were placed in the middle of the polystyrene wall. The first one, called top-middle temperature sensor, is inserted from the top of the sample, while the other one, called side-middle temperature sensor, is inserted from the left side of the sample. The aim of these two measurements is to scan the impact of the temperature sensor implementation on the measurement accuracy. The hemp concrete wall is instrumented with three internal temperature and relative humidity sensors, localized at the coating-wall interface (denoted by T_E), and at 3cm and 7cm from this interface (respectively denoted by T_1 and T_2). The sensors were inserted from the top of the wall through a hole which were made after its setting. This option was preferred to the introduction of the sensors during the manufacturing process to avoid any condensation issues within the sensors active cell. In addition, an attempt was made to measure the water content of the wall with TDR sensors following the approach presented in (Chabriac et al., 2005). However, the interference noise was found to be of the same order of magnitude as the signal variation due to the water content modification. For this experiment, their use does not appear optimal in the case of hygroscopic material, but more studies are needed on that point to draw a definitive conclusion. Finally, on both surfaces of each wall, incoming heat flux and temperatures were measured. The average value of the heat flux is denoted by q, while the surface temperatures are denoted by T_{sL} for the left surface and T_{sR} for the right surface.

3 Temperature and heat flux measurements

3.1 Measurement of the thermal conductivity

Assuming that the thermal behavior of the wall is under a pseudo-static state, the thermal conductivity can be measured through the relation:

$$\lambda = \frac{q\, l_{ij}}{T_i - T_j} \qquad (1)$$

where λ is the thermal conductivity of the material in $W{\cdot}m^{-1}{\cdot}K^{-1}$; q the measured thermal flux at the surface(s) in $W{\cdot}m^{-2}$; T_i and T_j and the measured temperatures at the locations i and j, while l_{ij} is the distance between i and j.

3.2 Impact of thermal bridge on measurements

The impact of the implementation of the temperature sensor on the measurement accuracy was studied on the polystyrene wallet. For that purpose, the thermal solicitation consists in imposing a temperature difference of 20°C between the two climatic chambers. To scan the reversibility of the measurements, two steps are considered. In the first one, the left chamber was hold at 40°C while the right one was hold at 20°C. In the second one, it was the opposite: 20°C for the left chamber and 40°C for the right one. The pseudo-static state was assumed to be reached when the values given by the two heat flow meters were constant and almost opposite from one surface to another. The thermal conductivity of the wall was then estimated trough the equation (1), for the two steps and considering the following five combinations of thermocouples:

- Middle from top - surface L: calculation made with the data of the temperature sensor inserted in the wall from its top and the left surface temperature sensor.
- Middle from top - surface R: calculation made with the data of the temperature sensor inserted in the wall from its top and the right surface temperature sensor.
- Middle from surface - surface L: calculation made with the data of the temperature sensor inserted in the wall from its right surface and the left surface temperature sensor.
- Middle from surface - surface R: calculation made with the data of the temperature sensor inserted in the wall from its right surface and the right surface temperature sensor.

- Surfaces R&L: calculation made with the data of the two surface temperature sensors.

The measurements are presented in Figure 2 and the deduced thermal conductivities are gathered in Table 1.

It can be noticed that the use of the sensor "middle from top" leads to a good estimation of the thermal conductivity of the wallet (error of less than 15% when compared to the value measured with the hot wire apparatus), and for both external surface (left or right) and the direction of the thermal gradient (from left to right or the opposite). The same observation can also be made for the two surface sensors. These results thus provide confidence on the setup protocol for the flow meters, and the temperature sensors.

On the contrary, a significant difference can be observed between the theoretical value of the thermal conductivity and the measurements of the temperature sensor called "middle from right surface". Indeed, looking at Figure 2, it can be noticed that the measured temperature is very close to the air temperature of the right side of the wallet, which suggests the presence of an important thermal bridge between the sensor and the climatic chamber. This leads to a decrease, almost divided by two, of the thermal conductivity in comparison with the one measured on the left surface, and an important increase (4 to 5 times) in comparison with the one measured on the right surface, from which the temperature sensor was inserted.

As a consequence, even if this experimental bias should be limited when the width of the wall increases, the sensor introduction along the thermal gradient propagation should be avoided as much as possible. In any case, every temperature measurement realized with this configuration should be interpreted taking into account this possible bias.

3.3 Impact of sensors locations within the wall

The investigation of the sensors locations within the wall was made on the hemp concrete wallet plastered with a mix of lime and sand. The measurements were realized considering two temperature steps. The "15-25" step has consisted in holding at 15°C the left climatic chamber while the right one was hold at 25°C. In the "30-40" step, the left chamber was at 30°C and the right one at 40°C. The pseudo-static state was assumed to be reached when the values given by the two heat flow meters were constant and almost opposite from one surface to another. The heat flux measured for these two steps at the pseudo-static state, as well as the data from all the temperature sensors (either at the surfaces or within the wallet) are reported in Table 2.

These values are then used to calculate the thermal conductivity through the relation (1). The results are gathered in Table 3.

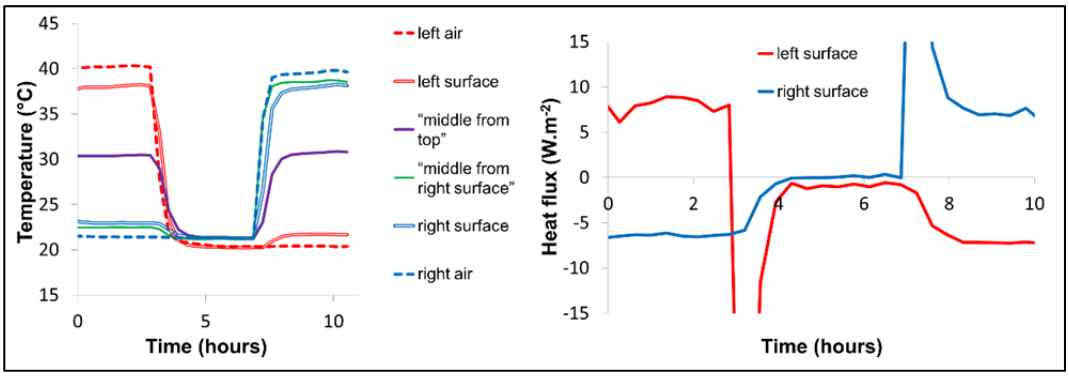

Figure 2. Results of the calibration test for the thermal conductivity evaluation on the polystyrene wallet. Left: Measurements of the temperature sensors. Right: Measurements of the heat flow meters.

Table 1. Calculation of the thermal conductivity for the polystyrene wallet, from different sensors and surfaces.

Sensors	Middle from top - surface				Middle from surface - surface				Surfaces R & L	
Steps	1		2		1		2		1	2
Surface	R	L	R	L	R	L	R	L	-	-
λ ($mW \cdot m^{-1} \cdot K^{-1}$)	30	40	30	30	193	19	184	16	35	30
Error (%)	14	15	13	13	452	44	424	53	1	13

Table 2. Measurements realized on the hemp concrete wallet in order to assess the thermal conductivity.

Steps	q ($W \cdot m^{-2}$)	T_{sL} (°C)	T_E (°C)	T_1 (°C)	T_2 (°C)	T_{sR} (°C)
15-25	9.3	16.0	16.1	18.5	21.3	23.4
30-40	9.3	30.9	31.1	33.3	36.1	38.1

Table 3. Calculation of the apparent thermal conductivity of hemp concrete and plaster by using the internal, surface and flow meter on the surface of the plaster. The "distance" line corresponds to the distance between the two sensors used to estimate the thermal conductivity. The error corresponds to the relative difference between the measured and reference values of the material, obtained by hot-wire tests.

	λ Hemp concrete ($mW \cdot m^{-1} \cdot K^{-1}$)				λ Plaster ($mW \cdot m^{-1} \cdot K^{-1}$)
Sensors	T_E, T_{sR}	T_E, T_2	T_1,T_2	T_E, T_1	T_{sL}, T_E
Distance (cm)	10	7	4	3	2
15-25	127	125	133	116	1860
Error (%)	2	4	2	11	86
30-40	129	125	132	116	930
Error (%)	1	4	2	11	7

No matter which combination is considered, the resulting thermal conductivity is equal to 130+/-20 $mW \cdot m^{-1} \cdot K^{-1}$ which is in the line with the value obtained with the hot wire apparatus. This result is not surprising since it is consistent with the pseudo-static state assumption. It gives nevertheless some confidence of the protocol used to insert the sensors within the wall. Regarding the plaster, the same comparison is made but the temperature difference between T_{sL} and T_E appears to be in the range of measurement uncertainties, and the methodology presented here was not able to reach the value of 1±0.1 $W \cdot m^{-1} \cdot K^{-1}$ obtained with the hot wire apparatus for the 15-25 step.

Note that these measurements were made on hemp mortar mixed in the laboratory and not on sprayed mortar, which leads to a better knowledge of the samples final density and enables a better comparison of the measurements between the wallet and the samples used with the hot wire apparatus.

3.4 Influence of the hygrothermal coupling on thermal measurements

Another aspect that has to be considered when dealing with such materials, is the hygrothermal coupling, i.e. the mutual influence of temperature and hygric states on thermal and hygric properties. For that purpose, a test was made on the hemp concrete wallet for which the left climatic chamber temperature was held at 30°C while the right one was held at 40°C. The two climatic chambers were initially at a relative humidity of 50%. After a stabilization period (of about one week), a sudden increase of relative humidity from 50% to 80% was performed in both climatic chambers. After another stabilization period of 8 days, a sudden decrease of relative humidity from 80% to 50% was imposed within both climatic chambers. The results were analyzed through the measurement of the global thermal transmittance of the wall, denoted by *U*, and equal to:

$$U = \left| \frac{q}{T_{left} - T_{right}} \right| \quad (2)$$

where T_{left} anf T_{right} are respectively the temperature within the left and the right climatic chambers.

The transmittance is key parameter for thermal assessment of buildings since it given a direct assessment of the global thermal performance of a wall. It is linked to the thermal conductivities of the elements composing the wall through the relation:

$$U = \left(R_{S,int} + \sum_i \frac{l_i}{\lambda_i} + R_{S,ext} \right)^{-1} \quad (3)$$

where $R_{S,int}$ and $R_{S,ext}$ are the thermal resistances of the wall surfaces, l_i is the thickness of the component *i* of the wall and λ_i is its thermal conductivity.

The protocol to properly measure the thermal transmittance of a wall is provided in the ISO 9869-1:2014 standard. The principle consists in measuring the heat flux at a surface of a wall as well as the temperature of the ambiances near the wall. This measurement must be made under a permanent (or pseudo-permanent) state. However, the measurement of thermal transmittance can happen to be more difficult for hygroscopic materials. Indeed, even if internal and external temperatures remain stable, relative humidity variations can induce parasite phenomena leading to a perturbation of the collected data. This phenomenon is illustrated in Figure 3. Indeed, before the increase of the relative humidity within the climatic chambers, the thermal transmittance of the 10cm-thick hemp concrete wallet is measured to be 1.2 $W \cdot m^{-2} \cdot K^{-1}$, which is quite consistent. However, just after the sudden increase of the relative humidity, a significant increase of the transmittance is observed (of about 60%) when the measurements are made using the heat flow meter located at the colder surface. The opposite was observed after the sudden decrease of relative humidity within the chambers. This is due to the hygrothermal processes occurring within the hemp concrete wallet, and in particular, the power supplied by the water adsorption process and the power consumed by the desorption process. This measurement thus underlines that the heat flux induced by the in-pore sorption/desorption processes is in the range of the one induced by a temperature difference of 10°C between the chambers for a plastered 10cm-thick hemp concrete wallet.

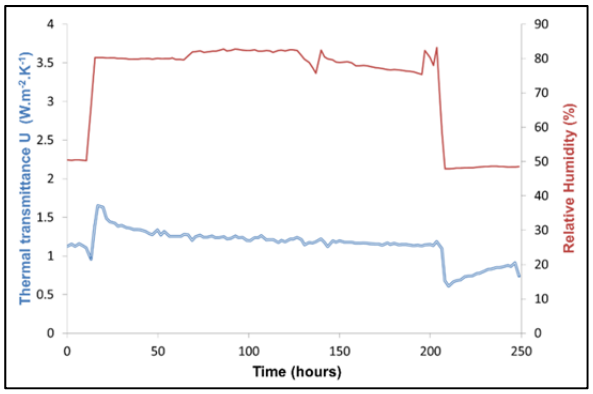

Figure 3. High variations in the thermal transmittance measurement following a change in relative humidity, in a 10cm width hemp mortar wallet

4 Concluding remarks on the instrumentation scheme

These different investigations enabled to draw some recommendations concerning the instrumentation scheme of hemp concrete walls, which is illustrated in the Figure 4.

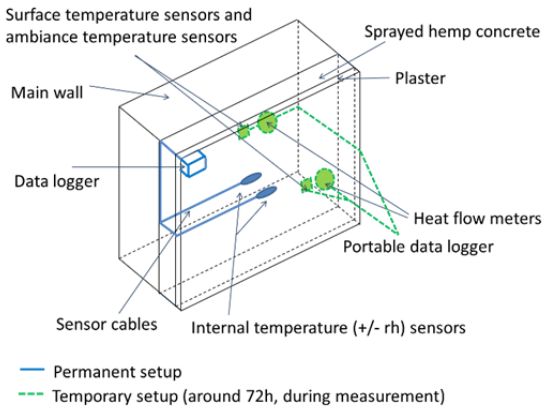

Figure 4. Schematic representation of the recommended placement for sensors to measure internal temperature

At first, the results show that the use of the flow meter and internal sensors is possible to estimate the thermal conductivity of hemp concrete. The value obtained with the sensor T1 (closest to the interface between the plaster and the hemp concrete) is the furthest from the reference value. In order to increase the precision of the measurements, it is therefore preferable to space as far as possible the two temperature sensors used. On the other hand, this study shows that, using this method, further analyses are needed to estimate the on-site thermal conductivity of the coating. Indeed, because of the great difference in thermal conductivity between the hemp mortar and the coating, the thermal gradient within this latter becomes very low. It follows that the difference between the temperature at the surface of the coating and that at the interface between the coating and the hemp concrete is of the same order of magnitude as the accuracy of the measurements. In any case, to reach consistent results, the placement of the internal temperature sensors directly from the external surfaces should be avoided.

In addition, this study underlines that the measurement protocol of the thermal transmittance must be modified for hygroscopic materials. To quantify the impact of hygrothermal effects on the measurement of thermal transmittance of the walls, a two-step method can be proposed. It consists in a first measurement on a wall subjected to low hydric variations in order to assess the "real" thermal transmittance in a steady-state case. Then, a second measurement should be performed on the same wall when subjected to its normal hydric variations. In this way, the evolution of thermal transmittance due to hygrothermal effect could be monitored. Note that, for both cases, temperatures have to remain reasonably stable from one side to the other side of the wall, which implies to protect from solar radiation.

At last, the investigation points developed in this study are part of the global goal described in the introduction, but further studies are needed to provide a complete instrumentation protocol for buildings monitoring. Among them, the question of measuring the hygric properties of these materials on site remains difficult as the effective thickness is only few centimeters. Anyway, regarding hygric monitoring, when possible, it is advised to place ducts within the wall in order to introduce relative humidity sensors after construction.

Acknowledgment

This present work has been supported by the French Agency for Environment and energy Management (ADEME) through project IBIS (PIA - Projets d'Investissement d'Avenir). The authors acknowledge ParexLanko for the supply of raw materials and for the realization of the sprayed hemp concrete samples, Frederic Sallet for the fabrication of the compacted hemp concrete samples and for insightful discussions on this topic.

References

[1] D. J. Harris, A quantitative approach to the assessment of the environmental impact of building materials. Build Environ (1999) 34: 751–758. https://doi.org/10.1016/S0360-1323(98)00058-4

[2] T. Pierre, T. Colinart, P. Glouannec, Measurment of thermal properties of biosourced building materials. Int J Thermophys (2014) 35: 1832–1852. https://doi.org/10.1007/s10765-013-1477-0

[3] F. Asdrubali, S. Schianoni, K. Horoshenkov, A review of sustainable materials for acoustic applications. Build Acoust (2012) 19: 283–311. https://doi.org/10.1260/1351-010X.19.4.283

[4] P. A. Chabriac, E. Gourdon, P. Gle, A. Fabbri, H. Lenormand, Agricultural by-products for building insulation : Acoustical characterization and modeling to predict micro-structural parameters. Constr Build Mater (2016) 112: 158–167. https://doi.org/10.1016/j.conbuildmat.2016.02.162

[5] P. Glé, E. Gourdon, L. Arnaud, Acoustical properties of materials made of vegetable particles with several scales of porosity. Appl Acoust (2011) 72: 249–259. https://doi.org/10.1016/j.apacoust.2010.11.003

[6] P. Walker, S. Pavia, Moisture transfer and thermal properties of hemp-lime concretes. Constr Build Mater (2014) 64: 270–276. https://doi.org/10.1016/j.conbuildmat.2014.04.081
[7] P. Jaquin, C. . Augarde, D. Gallipoli, D. G. Toll, The strength of unstabilised rammed earth materials. Geotechnique (2009) 59: 487–490. https://doi.org/10.1680/geot.2007.00129
[8] Q. Bui, J. Morel, S. Hans, P. Walker, Effect of moisture content on the mechanical characteristics of rammed earth. Constr Build Mater (2014): 163–169. https://doi.org/10.1016/j.conbuildmat.2013.12.067
[9] F. Champiré, A. Fabbri, J. Morel, H. Wong, F. Mcgregor, Impact of relative humidity on the mechanical behavior of compacted earth as a building material. Constr Build Mater (2016) 110: 70–78. https://doi.org/10.1016/j.conbuildmat.2016.01.027
[10] P. Gerard, M. Mahdad, A.R. McCormack, B. François, A unified failure criterion for unstabilized rammed earth materials upon varying relative humidity conditions. Constr Build Mater (2015) 95: 437-447. https://doi.org/10.1016/j.conbuildmat.2015.07.100
[11] F. Mcgregor, A. Heath, A. Shea, The moisture buffering capacity of unfired clay masonry. Build Environ (2014) 82: 599–607. https://doi.org/10.1016/j.buildenv.2014.09.027
[12] A. Arundel, E. Sterling, J. Biggin, Indirect health effect of relative humidity in indoor environments. Environ Health Perspect (1986) 65: 351-361.
[13] I. Gomes, T. D. Gonçalves, P. Faria, Hygric Behavior of Earth Materials and the Effects of their Stabilization with Cement or Lime: Study on Repair Mortars for Historical Rammed Earth Structures. J Mater Civ Eng (2016) 28: 04016041. https://doi.org/10.1061/(ASCE)MT.1943-5533.0001536
[14] L. Fang, G. Clausen, P. O. Fanger, Impact of temperatre and humidity on chemical and sensory emissions from building materials. Indoor Air (1999) 9: 193–201. https://doi.org/10.1111/j.1600-0668.1999.t01-1-00006.x
[15] M. Woloszyn, T. Kalamees, M. O. Abadie, M. Steeman, A. Kalagasidis, The effect of combining a relative-humidity-sensitive ventilation system with the moisture-buffering capacity of materials on indoor climate and energy efficiency of buildings. Build Environ (2009) 44: 515–524. https://doi.org/10.1016/j.buildenv.2008.04.017
[16] F. Collet, Thermal conductivity of hemp concretes: variation with formulation, density and water content. Constr Build Mater (2014) 65: 612–619. https://doi.org/10.1016/j.conbuildmat.2014.05.039
[17] H. Janssen, B. Blocken, J. Carmeliet, Conservative modelling of the moisture and heat transfer in building components under atmospheric excitation (post print). Int J Heat Mass Transf (2007) 50: 1128–1140. https://doi.org/10.1016/j.ijheatmasstransfer.2006.06.048
[18] L. Soudani, A. Fabbri, J.-C. Morel, M. Woloszyn, P.-A. Chabriac, A.-C. Grillet, Assessment of the validity of some common assumptions in hygrothermal modeling of earth based materials. Energy Build (2016) 116: 498-511. https://doi.org/10.1016/j.enbuild.2016.01.025
[19] C.-E. Hagentoft, A. Kalagasidis, B. Adl-Zarrabi, S. Roels, J. Carmeliet, H. Hens, Assessment method of numerical prediction models for combined heat, air, and moisture transfer in building components: benchmarks for one-dimensional cases. J Therm Envel Build Sci (2004) 27: 327–352. https://doi.org/10.1177/1097196304042436
[20] P. Taylor, R. Fuller, M. B. Luther, Energy use and thermal comfort in a rammed earth office building. Energy Build (2008) 40: 793–800. https://doi.org/10.1016/j.enbuild.2007.05.013
[21] D. Allinson M. R. Hall, Hygrothermal analysis of a stabilised rammed earth test building in the UK. Energy Build (2010) 42: 845–852. https://doi.org/10.1016/j.enbuild.2009.12.005
[22] C. Beckett, D. Ciancio, C. Huebner, R. Cardell-oliver, Sustainable and affordable rammed earth houses in Kalgoorlie, western Autralia : development of thermal monitoring techniques. Proceedings of ASEC 2014 (2014).
[23] L. Soudani, M. Woloszyn, A. Fabbri, J.-C. Morel, A.-C. Grillet, Assessment of solar heat gain for rammed earth walls from long term in-situ measurement. Build Environ (2017) submitted.
[24] F. Mcgregor, A. Fabbri, J. Ferreira, T. Simoes, P. Faria, J. Morel, Procedure to determine the impact of the surface film resistance on the hygric properties of composite clay/fibre plasters. Mater Struct (2017) 50: 193. https://doi.org/10.1617/s11527-017-1061-3
[25] H. M. Künzel, Simultaneous heat and moisture transport in building components one - and two-dimensional calculation using simple parameters - Report on PhD thesis, Fraunhofer Institute of Building Physics, 1995.
[26] A. Fabbri, F. Sallet, H. Wong, J.-C. Morel, Hygrothermal behaviour of hemp concrete: experimental evidences and modelling, VI International Conference on Computational Methods for Coupled Problems in Science and Engineering, 2015, 4.